PERGAMON

International Journal of Heat and Mass Transfer 45 (2002) 1033–1044

International Journal of HEAT and MASS TRANSFER

www.elsevier.com/locate/ijhmt

Saturated flow boiling heat transfer and pressure drop of refrigerant R-410A in a vertical plate heat exchanger

Y.Y. Hsieh, T.F. Lin *

Department of Mechanical Engineering, National Chiao Tung University, 1001 Ta Hsueh Road, Hsinchu 30010, Taiwan, ROC

Received 25 December 2000; received in revised form 30 June 2001

Abstract

Saturated flow boiling heat transfer and the associated frictional pressure drop of the ozone friendly refrigerant R-410A (a mixture of 50 wt% R-32 and 50 wt% R-125) flowing in a vertical plate heat exchanger (PHE) are investigated experimentally in the study. In the experiment two vertical counter flow channels are formed in the exchanger by three plates of commercial geometry with a corrugated sinusoidal shape of a chevron angle of 60°. Upflow boiling of saturated refrigerant R-410A in one channel receives heat from the downflow of hot water in the other channel. The experimental parameters in this study include the refrigerant R-410A mass flux ranging from 50 to 125 kg/m^2 s and imposed heat flux from 5 to 35 kW/m^2 for the system pressure fixed at 1.08, 1.25 and 1.44 MPa, which respectively correspond to the saturated temperatures of 10, 15 and 20 °C. The measured data showed that both the boiling heat transfer coefficient and frictional pressure drop increase almost linearly with the imposed heat flux. Furthermore, the refrigerant mass flux exhibits significant effect on the saturated flow boiling heat transfer coefficient only at higher imposed heat flux. For a rise of the refrigerant pressure from 1.08 to 1.44 MPa, the frictional pressure drops are found to be lower to a noticeable degree. However, the refrigerant pressure has very slight influences on the saturated flow boiling heat transfer coefficient. Finally, empirical correlations are proposed to correlate the present data for the saturated boiling heat transfer coefficients and friction factor in terms of the Boiling number and equivalent Reynolds number.

1. Introduction

Plate heat exchangers (PHEs) have been widely used in food processing, chemical reaction processes and many other industrial applications due to their high effectiveness, compactness, flexibility, and cost competitiveness. Furthermore, they have been introduced to the refrigeration and air conditioning systems as evaporators or condensers for their high efficiency and compactness. Recently, a number of investigations on PHE were reported in the open literature. Unfortunately, most studies about PHE in the open literature were mainly focused on the single-phase liquid-to-liquid heat transfer, especially for water [1–3]. There are rather limited data available for the design of PHEs used as evaporators and condensers. Recently, Yan and Lin [4,5] experimentally measured the evaporation and condensation heat transfer coefficients and frictional pressure drops for R-134a in a PHE. They showed that the evaporation heat transfer for R-134a flowing in the PHE was much higher than that in circular tubes, and both the evaporation heat transfer coefficient and pressure drop increased with the vapor quality. Moreover, the rise in the heat transfer coefficient with the vapor quality was larger than that in the pressure drop.

Over the past decades the hydrochlorofluorocarbon (HCFC) refrigerant R-22 has been used as the working fluid in many air-conditioning systems. But it will be phased out in a short period of time (before 2020) because of its high ozone depletion potential (ODP) and comparatively high global warming potential (GWP). As a result, the search for a replacement for R-22 has been intensified in recent years. Owing to the fact that

* Corresponding author. Tel.: +886-35-712121; fax: +886-35-720634.

E-mail address: t7217@cc.nctu.edu.tw (T.F. Lin).

0017-9310/02/$ - see front matter
PII: S0017-9310(01)00219-8

Nomenclature

A	heat transfer area of the plate, m^2
b	channel spacing, m
Bo	boiling number, $Bo = q/Gi_{fg}$, dimensionless
C_p	specific heat, J/kg °C
D_h	hydraulic diameter, m
f	friction factor in Eq. (22), dimensionless
g	acceleration due to gravity, m/s^2
G	mass flux, kg/m^2 s
G_{eq}	equivalent all liquid mass flux in Eq. (28)
h	heat transfer coefficient, W/m^2 °C
i_{fg}	enthalpy of vaporization, J/kg
k	thermal conductivity, W/m °C
L	channel length from center of inlet port to center of exit port, m
LMTD	log mean temperature difference, °C
P	system pressure, MPa
Pr	Prandtl number, $Pr = \mu C_p/k$, dimensionless
q	average imposed heat flux, W/m^2
Q	heat transfer rate, W
R_{wall}	thermal resistance of the wall
Re	Reynolds number, $Re = GD_h/\mu$, dimensionless
Re_{eq}	equivalent all liquid Reynolds number in Eq. (27)
T	temperature, °C
U	overall heat transfer coefficient, W/m^2 °C
u	flow velocity, m/s
v	specific volume m^3/kg
w	width of the plate, m
W	mass flow rate, kg/s
X	vapor quality

Greek symbols

ΔP	pressure drop, Pa
ΔT	temperature difference, °C
ΔX	quality change in the exchanger
ρ	density, kg/m^3
μ	viscosity, N s/m^2

Subscripts

a	acceleration
ave	average
ele	elevation
exp	experiment
f	friction
fg	difference between liquid phase and vapor phase
i, o	at inlet and exit of test section
l, g	liquid and vapor phase
m	average value for the two-phase mixture or between the inlet and exit
man	the test section inlet and exit manifolds and ports
r	refrigerant
sat	saturated state
w	water
wall	wall of the plate heat exchanger
tp	two-phase

there are no single-component HFCs which have thermodynamic properties close to those of R-22, binary or ternary refrigerant mixtures have been introduced. The alternative refrigerants evaluation program (AREP) technical committee has established an updated list of the potential alternatives to R-22. Some of the alternatives on the AREP's list are R-410A, R-410B, R-407C and R-507. Among the various alternatives to R-22, three refrigerants are gaining most favorable support depending on application and system design [6]: a look-alike zeotropic mixture such as 407C, higher pressure, nearly azeotropic mixtures like R-410A or R-410B, and the lower pressure refrigerant R-134a. Some studies were carried out and reported in the literature dealing with the subcooled flow boiling, saturation flow boiling, evaporation and condensation heat transfer of R-134a in ducts of various test section geometries, including smooth and micro-fin tubes, plate heat exchanger and the other enhanced heat transfer tubes for refrigerant R-134a [4,5,7–10]. However, the two-phase heat transfer characteristics for R-407C [11–15] and R-410A [16–21] flow in ducts are less examined.

In the following the relevant literature on the boiling heat transfer for R-410A is briefly reviewed. It should be mentioned here that the refrigerant R-410A is a mixture of 50 wt% R-32 and 50 wt% R-125 which exhibits azeotropic behavior. Sami and Poirier [16] compared the evaporation and condensation heat transfer data for several refrigerant blends proposed as substitutes for R-22, including R-410A, R-410B, R-507 and the quaternary mixture R-32/125/143a/134a inside enhanced-surface tubing. They showed that the two-phase heat transfer coefficients and pressure drops increased with the refrigerant mass flux for all alternative refrigerants and R22. In a continuing study [17], they presented the data for R-410A and R-507 in a double fluted tube indicating that for the refrigerant Reynolds number higher than 4.2×10^6, R-410A had a greater heat transfer rate than that of R-507. Wang et al. [18] tested nucleate boiling on several commercially available enhanced-surface tubes to assess the pool boiling heat transfer performance for R-22, R-123, R-134a, R-407C, and R-410A. The heat transfer coefficient of R-410A was found to be higher than that of R-22 for most enhanced tubes.

This outcome was attributed to the higher latent heat, thermal conductivity and specific heat for R-410A and the corresponding liquid viscosity was lower. Ebisu and Torikoshi [19] measured the evaporation heat transfer coefficient and proposed empirical correlations for R-410A, R-407C and R-22 flowing inside a horizontal smooth tube. Their results showed that the evaporation heat transfer coefficient of R-410A was 20% higher than that of R-22 up to the quality of 0.4, while the heat transfer coefficients for both R-410A and R-22 became almost the same at the quality of 0.6. Furthermore, the pressure drop for R-410A was about 30% lower than that of R-22 during evaporation. The quantitative differences in the pressure drops between R-410A and R-22 were mainly attributed to the differences in vapor density of two refrigerants. The greater the vapor density, the smaller the pressure drop of a refrigerant. A similar study was carried out by Wijaya and Spatz [20] for refrigerants R-22 and R-410A in a horizontal smooth copper tube. Their data showed that the evaporation heat transfer coefficients for R-410A were much higher (about 23–63%) than those for R-22, while the R-410A pressure drops were 23–38% lower than those for R-22. The advantageous heat transfer characteristics and pressure drops for R-410A were ascribed to the better transport properties for R-410A. Shen et al. [21] provided the data for the pool boiling heat transfer coefficient of the binary mixture R-32/R-125 with different mole fractions of R-32. The results indicated that the pressure and the heat flux dependence of the heat transfer coefficient for the R-32/R-125 mixtures did not significantly differ from those of pure components.

The above literature review clearly reveals that heat transfer in PHE has been studied mainly for single-phase flow, especially for water. Very few data are available for the phase change heat transfer characteristics associated with the PHEs. Although R-410A is one of the most likely substitute for R-22, the two-phase heat transfer data for R-410A are still scarce. To continue our previous study on the phase change heat transfer for R-134a in PHE [4,5], the saturated flow boiling heat transfer characteristics and pressure drops for refrigerant R-410A flow in a vertical PHE are investigated experimentally in this study. In addition, empirical correlations will be developed for predicting the corresponding heat transfer coefficient and friction factor for R-410A boiling in the PHE.

2. Experimental apparatus and procedures

The experimental apparatus established in the present study to investigate the saturated flow boiling heat transfer of R-410A in a vertical PHE, as

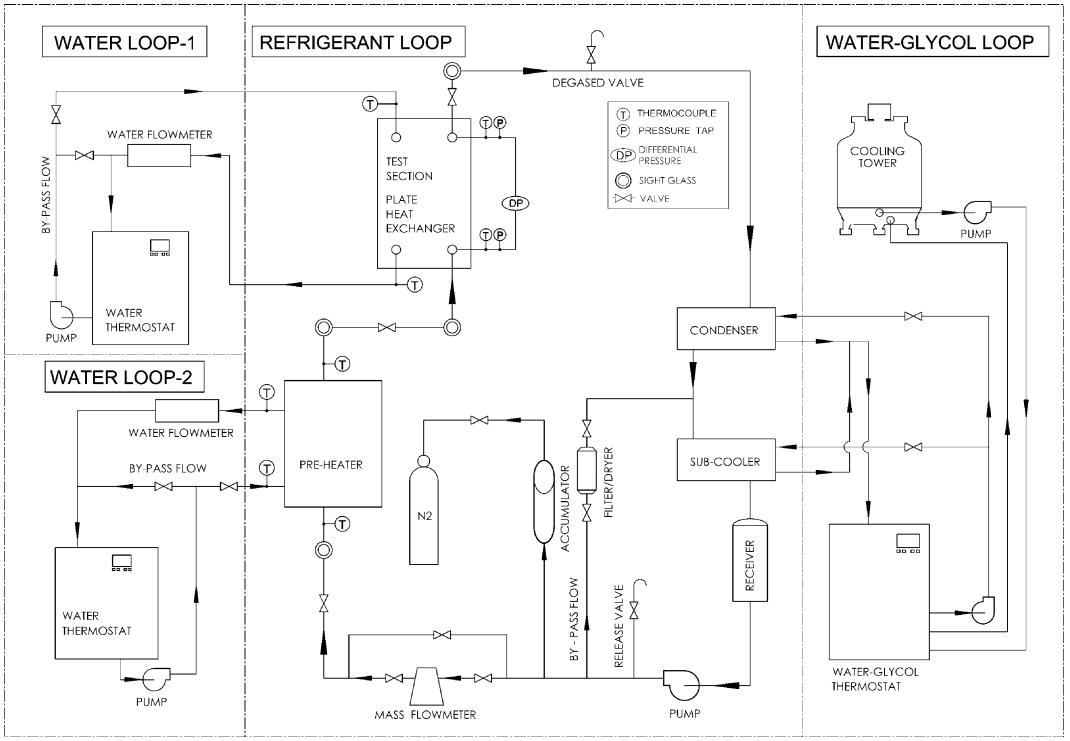

Fig. 1. Schematic diagram of the experimental system.

schematically shown in Fig. 1, consists of four independent loops and a data acquisition system. It includes a refrigerant loop, two water loops (one for preheater and the another for the test section), and a cold water–glycol loop. In order to control various test conditions of R-410A (including imposed heat flux, refrigerant mass flux and system pressure) in the test section, we need to control the temperature and flow rate in the other three loops.

2.1. Refrigerant flow loop

The refrigerant loop contains a variable-speed refrigerant pump that delivers the subcooled refrigerant to a preheater. The refrigerant mass flow rate is mainly controlled by an AC motor through the change of the inverter frequency. The flow rate can be further adjusted by regulating the bypass valve in the flow path from the refrigerant pump. To measure the refrigerant mass flow rate, an accurate mass flux meter is installed between the refrigerant pump and preheater with a reading accuracy of ±1%. The subcooled refrigerant liquid is heated in the preheater to a prescribed saturated state before entering the test section. Then, the saturated liquid refrigerant moves into the test section and R-410A boils there. Finally, the vapor–liquid refrigerant mixture is condensed and subcooled by the low-temperature water–glycol in the shell-and-coil heat exchangers acting as condenser and subcooler. An accumulator is connected to a high-pressure nitrogen tank to dampen the fluctuations of the flow rate and pressure. In addition, the loop is also equipped with a receiver, a filter/dryer, a release valve, a degassed valve and four sight glasses. The pressure of the refrigerant loop can be controlled by varying the temperature and flow rate of the water–glycol in the condenser and subcooler. Two absolute pressure transducers are installed at the inlet and exit of the test section with resolution up to ±2 kPa. Furthermore, a calibrated differential pressure transducer is used to measure the overall pressure drop across the refrigerant side of the vertical PHE. All the water and refrigerant temperatures are measured by type T copper–constantan thermocouples with a calibrated accuracy of ±0.2 °C. A 5 cm thick polyethylene insulation is wrapped around the whole loop to reduce the heat loss to the ambient.

2.2. PHE

Three commercial SS-316 plates manufactured by the Kaori Heat Treatment, Taiwan form the PHE for the saturated flow boiling test. The plate surfaces are pressed to become grooved with a corrugated sinusoidal shape and 60° of chevron angle, which is the angle of V-grooves to the vertical axis of the plate. The detailed configuration for the PHE can be seen in Fig. 2. The corrugated grooves on the right and left outer plates

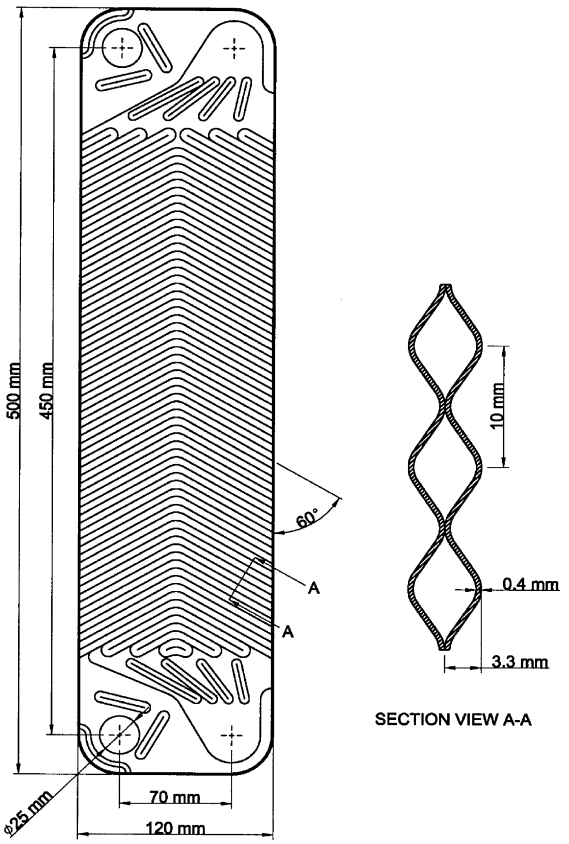

Fig. 2. Schematic diagram of PHE.

have a V shape but those in the middle plate have a contrary V shape on both sides. This arrangement allows the flow stream to be divided into two different flow directions along the plates. Thus, the flow moves mainly along the grooves in each plate. Due to the contrary V shapes between two neighbor plates the flow streams near the two plates cross each other in each channel. This cross flow results in significant flow unsteadiness and randomness. In fact, the flow is highly turbulent even when the Reynolds number is low. In the PHE three plates form two vertical counter flow channels. Upflow of the saturated refrigerant R-410A in one channel is heated by the downflow of the hot water in the other channel. The heat transfer rate in the test section is calculated by measuring the water temperature drop between the water channel inlet and outlet and the water flow rate.

2.3. Water loop for test section

The water loop in the experimental system for circulating the hot water through the test section contains a 20 l water thermostat with a 0.5 kW heater, and a water pump is used to drive the hot water at a specified water

flow rate. A by-pass valve can also be used to adjust the water flow rate. The accuracy of measuring the water flow rate is ±0.5%.

2.4. Water loop for preheater

Another water loop designed for the preheater consists of a 125 l hot water thermostat and a water pump which drives the hot water at specified temperature and flow rate to the preheater. Similarly, a by-pass valve is also used to adjust the flow rate.

2.5. Water–glycol loop

Both the condenser and subcooler, which respectively condenses and subcools the refrigerant R-410A leaving the test section, are cooled by an independent low-temperature water–glycol loop. The cooling capacity is 3.5 kW for the water–glycol at −20 °C. A 0.5 hp pump is used to drive the water–glycol at a specified flow rate to the condenser as well as to the subcooler. A by-pass valve is also provided to adjust the flow rate.

2.6. Data acquisition

The data acquisition system includes a recorder, a 24 V–3 A power supply, and a controller. The water flowmeter and differential pressure transducer use the power supply as a driver to output an electric current of 4 to 20 mA. The data signals are collected and converted by a data acquisition system (Hybrid recorder). The converted signals are then transmitted to a host computer through a GPIB interface for further calculation.

2.7. Experimental procedures

In each test the R-410A pressure at the test section inlet is first maintained at the saturated level by adjusting the water–glycol temperature and flow rate through the condenser and subcooler. Then, the temperature and flow rate of the hot water loop for the preheater are adjusted to keep the R-410A at the saturated liquid state. Next, the heat transfer rate between the counterflow channels in the test section can be varied by changing the water temperature and flow rate in the water loop for the test section. Meanwhile, by selecting the frequency of the inverter connecting to the refrigerant pump and by adjusting the by-pass valve, the R-410A flow rate in the test section is maintained at a desired value.

In the test any changes of the system variables will lead to fluctuations in the temperature and pressure of the refrigerant flow. It takes about 20–100 min for the system to reach a statistically stable state at which variations of the time-average inlet and outlet temperatures are both less than ±0.2 °C, and the variations of the pressure and imposed heat flux are within 1% and 4%, respectively. Then the data acquisition unit is initiated to scan all the data channels for 10 times in 50 s. The mean value of the data for each channel is used to calculate the boiling heat transfer coefficient and pressure drop. Additionally, the flow rate of water in the test section should be high enough to have turbulent flow in the water side so that the associated single-phase heat transfer in it is high enough for balancing the boiling heat transfer in the refrigerant side. In this study, the Reynolds number of the water flow is maintained beyond 200.

Before examining the R-410A saturated flow boiling heat transfer characteristics, a preliminary test for single-phase water-to-water convective heat transfer in the PHE is performed. The Wilson's method [22] is adopted to calculate the relation between the single-phase heat transfer coefficient and the flow rate from these data. The single-phase heat transfer coefficient can then be used to analyze the data acquired from the saturated flow boiling heat transfer experiments. In order to correlate the data for the R-410A saturated flow boiling heat transfer coefficient, single-phase heat transfer tests of liquid R-410A are also performed.

2.8. Uncertainty analysis

The uncertainties of the experimental results are analyzed by the procedures proposed by Kline and McClintock [23]. The detailed results from the present uncertainty analysis for the experiments conducted here are summarized in Table 1.

3. Data reduction

A data reduction analysis is needed in the present measurement to deduce the boiling heat transfer coefficient from the measured heat transfer data. From the definition of the hydraulic diameter, Shah and Focke [24] suggested the use of two times the mean channel spacing as the hydraulic diameter for the PHE when the channel width is much larger than the channel spacing, i.e.

$$D_h \cong 2b \quad \text{for } w \gg b. \tag{1}$$

Saturated flow boiling heat transfer coefficient and the associated pressure drop are calculated from reducing the measured raw data in a computer program. The reduction procedures are described in the following sections.

3.1. Single-phase heat transfer

In the single-phase liquid water-to-liquid refrigerant heat transfer tests, the energy balance between the water and refrigerant sides was found to be within 2.0% for all runs. That is

Table 1
Summary of the uncertainty analysis

Parameter	Nominal values	Uncertainty
PHE geometry		
Length, width and thickness	500, 120, 0.4 mm	±0.00005 m
Area of the plate	0.064 m^2	$\pm 7 \times 10^{-5}$ m^2
Sensors		
Temperature, T	7.5–30.5 °C	±0.2 °C
Temperature difference, ΔT	0.2–9.6 °C	±4.5%
System pressure, P	1.05–1.45 MPa	±0.002 MPa
Pressure drop, ΔP	4000–11 500 Pa	±200 Pa
Water flow rate, W_w	1.60–2.85 l/m	±2%
Mass flux of refrigerant, G	50–125 kg/m^2 s	±2%
Single-phase heat transfer		
Heat transfer rate, Q	200–2500 W	±6.5%
Heat transfer coefficient, h_w	950–3850 W/m^2 °C	±11.0%
Heat transfer coefficient, $h_{r,l}$	2000–5000 W/m^2 °C	±12.5%
Saturated flow boiling heat transfer		
Boiling heat flux, q	3.2–38.5 kW/m^2	±8.5%
Heat transfer coefficient, $h_{r,sat}$	3200–8400 W/m^2 °C	±14.5%
Friction factor	0.86–4.35	±16.5%

$$\frac{|Q_w - Q_r|}{Q_{ave}} \leqslant 2.0\%, \tag{2}$$

where

$$Q_w = W_w C_{p,w}(T_{w,i} - T_{w,o}), \tag{3}$$
$$Q_r = W_r C_{p,r}(T_{r,o} - T_{r,i}), \tag{4}$$
$$Q_{ave} = (Q_w + Q_r)/2. \tag{5}$$

The thermodynamic and transport properties of water and R-410A are calculated according to the averages of the test section inlet and outlet temperatures. The overall heat transfer coefficient U_l between the two counter channel flows is then calculated from

$$U_l = \frac{Q_{ave}}{A\,\mathrm{LMTD}} \tag{6}$$

where A is the heat transfer area accounting for the actual corrugated surface of the plate which can be found from the design data provided by the manufacturer. The log mean temperature difference (LMTD) is determined from

$$\mathrm{LMTD} = \frac{(\Delta T_1 - \Delta T_2)}{\ln(\Delta T_1/\Delta T_2)}, \tag{7}$$

where

$$\Delta T_1 = T_{w,i} - T_{r,o}, \quad \Delta T_2 = T_{w,o} - T_{r,i}. \tag{8}$$

In view of the same heat transfer area in the refrigerant and water sides, the relation between the overall heat transfer and convection heat transfer coefficients on both sides can be expressed as:

$$\frac{1}{h_{r,l}} = \frac{1}{U_l} - \frac{1}{h_w} - R_{wall}A, \tag{9}$$

where $h_{r,l}$ and h_w are, respectively, the heat transfer coefficients for the single-phase liquid refrigerant R-410A and water, and $R_{wall}A$ is the wall thermal resistance. To obtain the single-phase R-410A convection heat transfer coefficient, the convection heat transfer coefficient in the water side needs to be determined first. This is accomplished by means of separate water-to-water tests in the same apparatus, combining with the subsequent Wilson-plot analyses of the measured data.

3.2. Saturated flow boiling heat transfer

The procedures to calculate the saturated boiling heat transfer coefficient of the refrigerant flow are described in the following. Firstly, the total heat transfer rate between the counter flows in the PHE is calculated from the hot water side

$$Q_w = W_w C_{p,w}(T_{w,i} - T_{w,o}). \tag{10}$$

Note that before entering the test section, the refrigerant flow is heated to the saturated liquid state from the heat transfer in the preheater. Then, the heat transfer from the hot water to the refrigerant sides in the test section causes the liquid refrigerant to boil. The change in the refrigerant vapor quality in the test section, ΔX, is then deduced from the heat transfer rate between the water and refrigerant sides in the test section Q_w:

$$\Delta X = X_o = \frac{Q_w}{i_{fg} W_r}. \tag{11}$$

Note that X_o estimated above can be qualitatively compared with that observed from the sight glass located at the exit end of the PHE (Fig. 1). The determination of the overall heat transfer coefficient for the saturated flow boiling of R-410A in the PHE is similar to that for the single-phase heat transfer, i.e.

$$U = \frac{Q_w}{A\,\mathrm{LMTD}}. \tag{12}$$

The LMTD is again calculated from

$$\mathrm{LMTD} = \frac{(\Delta T_1 - \Delta T_2)}{\ln(\Delta T_1/\Delta T_2)} \tag{13}$$

here for the saturated boiling

$$\begin{aligned} \Delta T_1 &= T_{w,i} - T_{r,sat}, \\ \Delta T_2 &= T_{w,o} - T_{r,sat}. \end{aligned} \tag{14}$$

Finally, the saturated flow boiling heat transfer coefficient in the flow of R-410A is evaluated from the equation

$$\frac{1}{h_{r,sat}} = \frac{1}{U} - \frac{1}{h_w} - R_{wall}A, \tag{15}$$

where h_w is determined from the empirical correlation for the single-phase water-to-water heat transfer test conducted in the present study.

3.3. Friction factor

To evaluate the friction factor associated with the R-410A saturated flow boiling, the frictional pressure drop ΔP_f is calculated by subtracting the acceleration pressure drop ΔP_a, the pressure losses at the test section inlet and exit manifolds and ports ΔP_{man}, and the elevation pressure rise ΔP_{ele} from the measured total pressure drop ΔP_{exp} in the refrigerant channel

$$\Delta P_f = \Delta P_{exp} - \Delta P_a - \Delta P_{man} - \Delta P_{ele}. \tag{16}$$

The acceleration pressure drop and elevation pressure rise are estimated by the homogeneous model for two-phase gas–liquid flow [25]

$$\Delta P_a = G^2 v_{fg} \Delta X, \tag{17}$$

$$\Delta P_{ele} = \frac{gL}{v_m}, \tag{18}$$

where v_m is the specific volume of the vapor–liquid mixture when the vapor and liquid are homogeneously mixed and is given as

$$v_m = [X_m v_g + (1 - X_m)v_l] = [v_l + X_m v_{fg}]. \tag{19}$$

The pressure drop in the inlet and outlet manifolds and ports was empirically suggested by Shah and Focke [24]. It is approximately 1.5 times the head due to flow expansion at the inlet

$$\Delta P_{man} \cong 1.5\left(\frac{u_m^2}{2v_m}\right)_i, \tag{20}$$

where u_m is the mean flow velocity. With the homogeneous model the mean velocity is

$$u_m = G v_m. \tag{21}$$

Based on the above estimation, the acceleration pressure drop ΔP_a and the pressure losses at the test section inlet and exit manifolds and ports ΔP_{man} are found to be rather small. In fact, the summation of the pressure losses ΔP_a and ΔP_{man} ranges from 1% to 3% of the total pressure drop. According to the definition

$$f_{tp} = -\frac{\Delta P_f D_h}{2G^2 v_m L} \tag{22}$$

the friction factor for the saturated flow boiling of R-410A in the PHE is obtained.

4. Results and discussion

In what follows selected results from the present measurement are presented to illustrate the saturated boiling heat transfer and frictional pressure drop of the R-410A flow in the vertical plate heat exchanger. Specifically, the data for the boiling heat transfer coefficient and frictional pressure drop in the flow affected by the refrigerant mass flux, system pressure (saturation temperature) and imposed heat flux are to be examined in detail. Furthermore, empirical correlation equations for the heat transfer coefficient and friction factor are proposed. In the present experiment the refrigerant mass flux G is varied from 50 to 125 kg/m^2 s, system pressure P from 1.08 to 1.44 MPa (saturated temperature T_{sat} from 10 to 20 °C), and imposed heat flux q from 5 to 35 kW/m^2. The range of the saturated temperature chosen here is suitable for the application encountered in air conditioning.

4.1. Single-phase heat transfer

Single-phase liquid R-410A convection heat transfer coefficients and frictional pressure drops are determined for the refrigerant inlet temperature ranging from 8 to 15 °C and mass flux from 50 to 200 kg/m^2 s (corresponding to the Reynolds number of 1500–6250). Fig. 3 shows the comparison of the present single-phase heat transfer data for R-410A with those for R134a from Chiang [26] in the PHE. The results showed that the single-phase R-410A heat transfer coefficients for both R-410A and R-134a increase with the Reynolds number. Besides, h_r for R-410A is about 25% to 35% higher than that for R-134a. The higher heat transfer coefficient for R-410A can be attributed mainly to the higher liquid thermal conductivity of R-410A. For instance, the physical

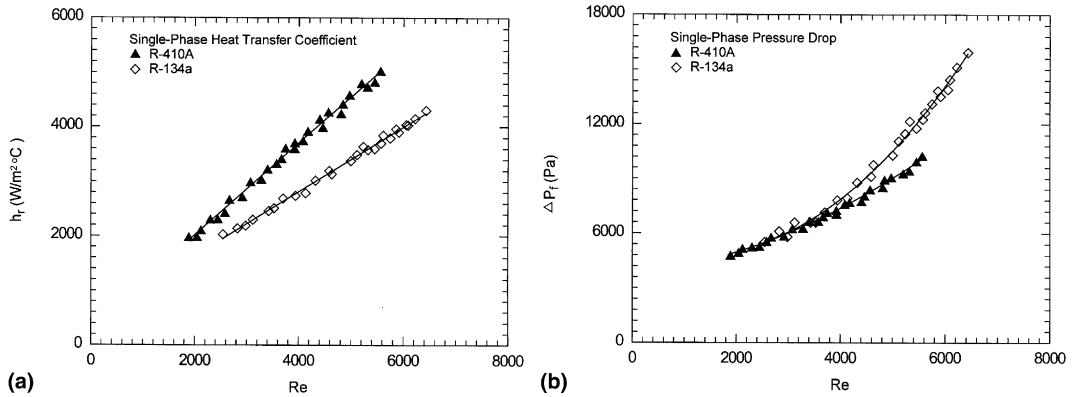

Fig. 3. Comparison of the present single-phase liquid data for: (a) heat transfer coefficient and (b) frictional pressure drop variations with Reynolds number for R-410A with those for R-134a from [26].

Table 2
Physical properties for R-410A and R-134a

	Temperature							
	5 °C		10 °C		15 °C		20 °C	
Refrigerant	R-410A	R-134a	R-410A	R-134a	R-410A	R-134a	R-410A	R-134a
ρ_l, kg/m^3	1150.9	1278.0	1129.4	1261.0	1107.8	1243.5	1086.3	1225.0
ρ_g, kg/m^3	35.9	17.14	42.5	20.23	49.1	23.8	55.6	27.78
μ_l, 10^{-6} Pa s	156.2	254.4	147.1	238.8	138.0	224.3	128.4	210.7
μ_g, 10^{-6} Pa s	12.6	11.0	13.0	11.5	13.2	11.4	13.6	11.58
$C_{p,l}$, kJ/kg °C	1.534	1.355	1.568	1.370	1.601	1.3865	1.635	1.405
$C_{p,g}$, kJ/kg °C	1.157	0.925	1.212	0.946	1.268	0.9725	1.323	1.001
i_{fg}, kJ/kg	214.8	217.4	208.1	211.7	201.5	205.6	194.8	198.9
k_l, W/m °C	0.1110	0.0912	0.1079	0.0089	0.1048	0.0087	0.1016	0.0084
k_g, W/m °C	0.0123	0.0122	0.0129	0.0127	0.0136	0.0131	0.0144	0.0136

properties listed in Table 2 for R-410A and R-134a show that at 15 °C the thermal conductivity of liquid R-410A is approximated 15% higher than that of R-134a. However, the density and viscosity of liquid R-410A is respectively about 15% and 60% lower than those of R-134a. Thus, the frictional pressure drop of liquid R-410A is lower than that for R-134a especially at high Reynolds numbers.

4.2. Saturated flow boiling heat transfer

The effects of the refrigerant mass flux, system pressure and imposed heat flux on the saturated boiling heat transfer coefficient of refrigerant R-410A in the vertical PHE are examined in the following. The measured experimental data are presented in Fig. 4 to first illustrate the changes of the R-410A saturated boiling heat transfer coefficient with the imposed heat flux for various mass fluxes and system pressures. These results indicate that at the low imposed heat flux the saturated flow boiling heat transfer coefficient is insensitive to the refrigerant mass flux. This can be ascribed to the fact that at the low imposed heat flux boiling in the liquid refrigerant is relatively weak due to the low wall superheat. Furthermore, at given G and P the boiling heat transfer coefficient increases almost linearly with the imposed heat flux. The increase is rather significant even at a low mass flux. For example, at $G = 50$ kg/m^2 s and $P = 1.08$ MPa the boiling heat transfer coefficient for $q = 35$ kW/m^2 is about 65% higher than that for $q = 5$ kW/m^2 (Fig. 4(a)). This large rise in the heat transfer coefficient is considered to mainly result from the higher nucleation density on the plate, higher bubble generation frequency and faster bubble growth for a higher imposed heat flux. In addition, it was found that even at a low imposed heat flux of 5 kW/m^2 the heat transfer coefficient is still maintained above 3300 W/m^2 °C. This is attributed to the contra V-grooves in the PHE which cause the flow to become highly turbulent and to the higher thermal conductivity of R-410A.

To be more specific on how the refrigerant mass flux affects the saturated flow boiling heat transfer coefficient, Fig. 5 shows the data for various mass fluxes at

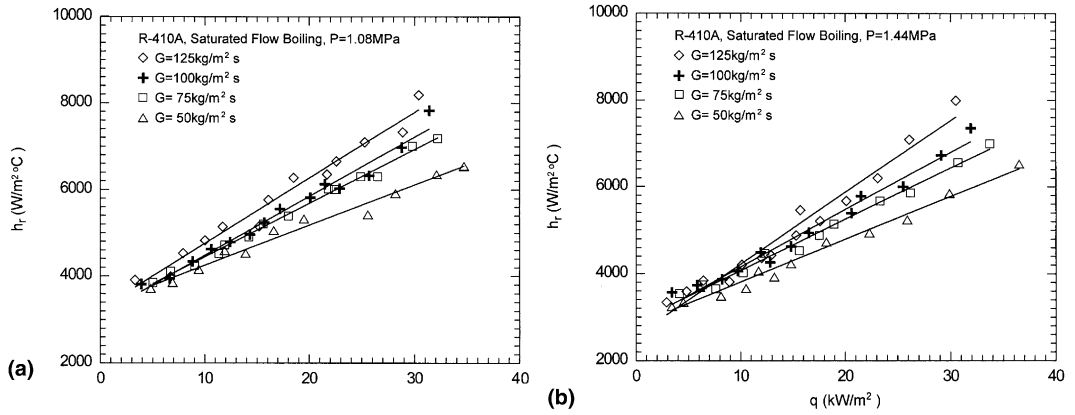

Fig. 4. Variations of the saturated flow boiling heat transfer coefficient with the imposed heat flux for various mass fluxes at: (a) $P = 1.08$ MPa; (b) 1.44 MPa.

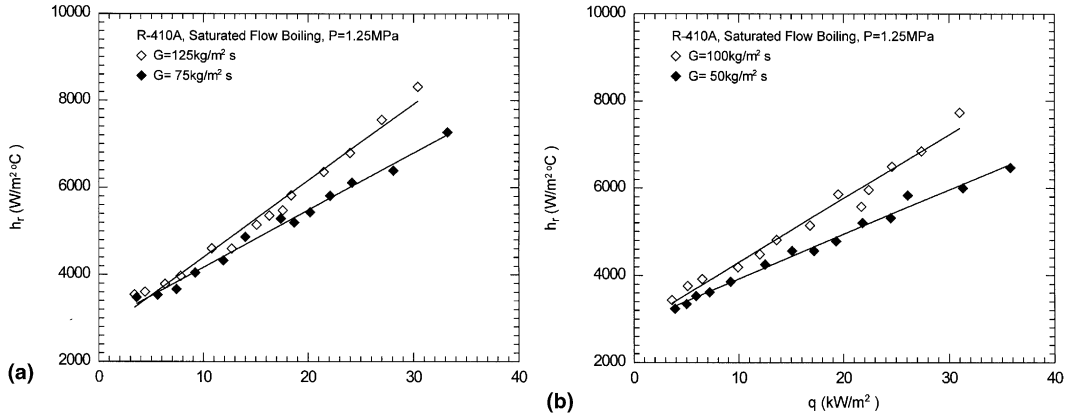

Fig. 5. Variations of the saturated boiling heat transfer coefficient with the imposed heat flux for various mass fluxes at $P = 1.25$ MPa and $G = 125$ and 75 kg/m^2 s (a) and 100 and 50 kg/m^2 s (b).

$P = 1.25$ MPa. As previously discussed, the saturated flow boiling heat transfer coefficient is insensitive to the change in the refrigerant mass flux at low imposed heat flux. However, the boiling heat transfer coefficient for the high mass flux of 125 kg/m^2 s rises much quicker than that for the low mass flux of 75 kg/m^2 s (Fig. 5(a)). For instance, the average h_r for $G = 125$ kg/m^2 s is about 35% higher than that for $G = 75$ kg/m^2 s. This result is the consequence of the stronger convection in the flow associated with the higher mass flux, which tends to cause the earlier departure of the bubbles on the plate and hence enhances the bubble generation frequency. A similar trend is noted for the lower refrigerant mass fluxes of 100 and 50 kg/m^2 s (Fig. 5(b)).

The effects of the system pressure of the refrigerant channel on the saturated boiling heat transfer are illustrated in Fig. 6 by comparing the data at the same mass flux for the three cases with the system pressures fixed at 1.08, 1.25 and 1.44 MPa, which are respectively equivalent to the saturated temperatures of 10, 15 and 20 °C for R-410A. These results indicate that the saturated flow boiling heat transfer coefficient is only slightly affected by the refrigerant pressure.

4.3. Frictional pressure drop

The variations of the frictional pressure drop in the saturated flow boiling of R-410A in the PHE with the imposed heat flux are shown in Figs. 7 and 8 for different mass fluxes and system pressures. As that for the saturated boiling heat transfer coefficient, the total frictional pressure drop in the PHE increases with the imposed heat flux for given mass flux and saturated pressure. It is further noted from the results that a higher mass flux results in a higher pressure drop. Moreover, at a higher imposed heat flux the mass flux effects are stronger. For

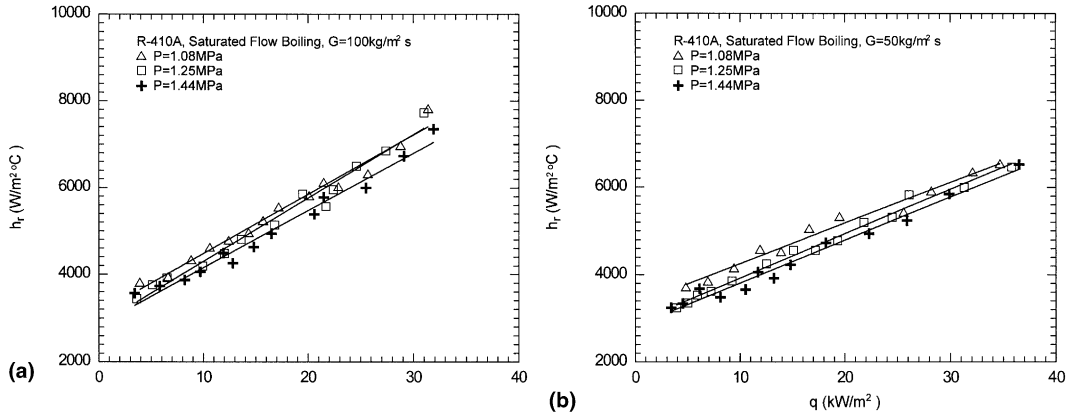

Fig. 6. Variations of the saturated boiling heat transfer coefficient with the imposed heat flux for various system pressures at: (a) $G = 100$ kg/m^2 s; (b) 50 kg/m^2 s.

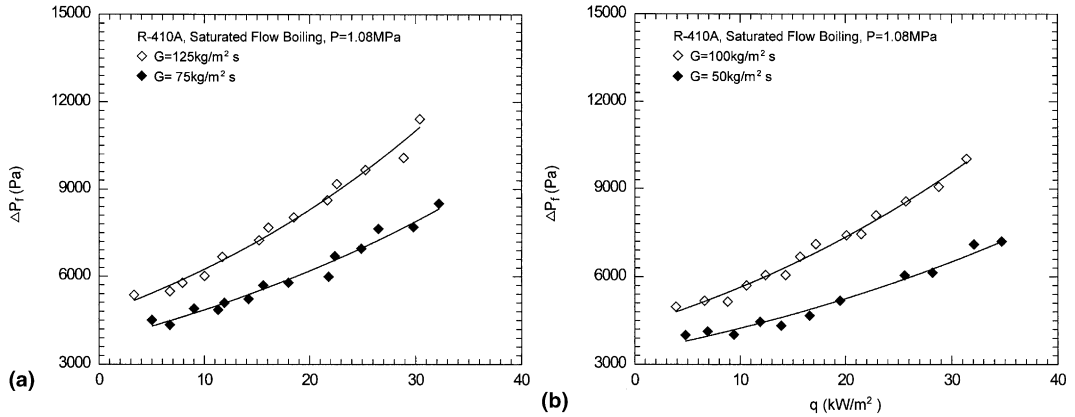

Fig. 7. Variations of the frictional pressure drop with the imposed heat flux for various mass fluxes at $P = 1.08$ MPa for: (a) $G = 125$ and 75 kg/ m^2 s; (b) $G = 100$ and 50 kg/m^2 s.

example, at $P = 1.08$ MPa and $G = 125$ kg/m^2 s the frictional pressure drop at the imposed heat flux of 30 kW/m^2 is about 60% higher than that at 5 kW/m^2 (Fig. 7(a)). But at $P = 1.08$ MPa and $G = 50$ kg/m^2 s the corresponding frictional pressure drop increase is only about 35% (Fig. 7(b)). Note that the frictional pressure drop reduces substantially for a rise of the system pressure from 1.08 to 1.44 MPa especially at a higher mass flux, as it is clear from the results in Fig. 8. For example, at $G = 100$ kg/m^2 s and $q = 20$ kW/m^2 the frictional pressure drop at the pressure of 1.08 MPa is about 10% and 22% higher than that at $P = 1.25$ and 1.44 MPa, respectively. The higher ΔP_f for a lower refrigerant pressure is attributed to the fact that for a lower system pressure (that is for lower saturation temperature) the specific volume of R-410A vapor and the viscosity of the liquid R-410A are higher. We further note that for most cases the rise in the saturated boiling heat transfer coefficient with the imposed heat flux is more prominent than that in the frictional pressure drop.

4.4. Correlation equations

Correlation equations for the heat transfer coefficient and frictional pressure drop associated with the saturated flow boiling of R-410A in the vertical PHE considered here are important in the design of highly energy efficient air conditioning and refrigeration systems. Based on the present data the boiling heat transfer coefficient can be correlated as

$$h_{r,sat} = h_{r,l}\left(88Bo^{0.5}\right), \tag{23}$$

where $h_{r,l}$ is the all-liquid nonboiling heat transfer coefficient and is determined from the empirical correlation for the present single-phase heat transfer tests for liquid R-410A as

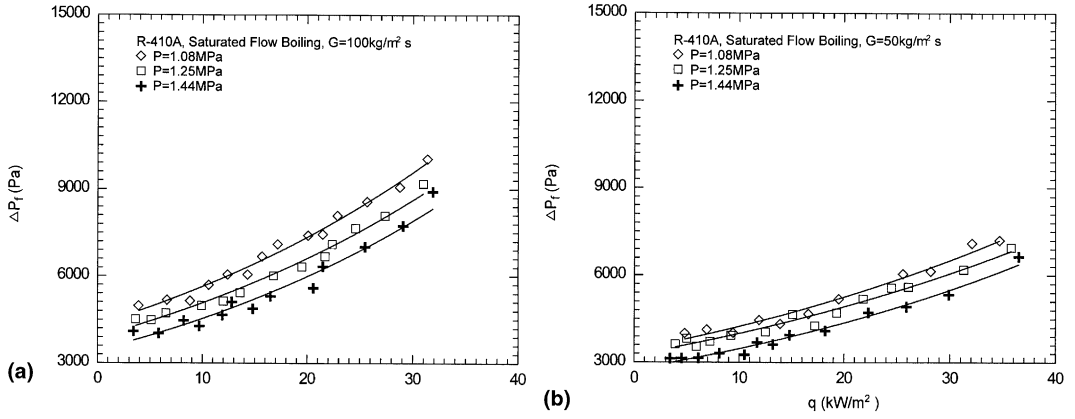

Fig. 8. Variations of the frictional pressure drop with the imposed heat flux for various system pressures at: (a) $G = 100$ kg/m^2 s; (b) 50 kg/m^2 s.

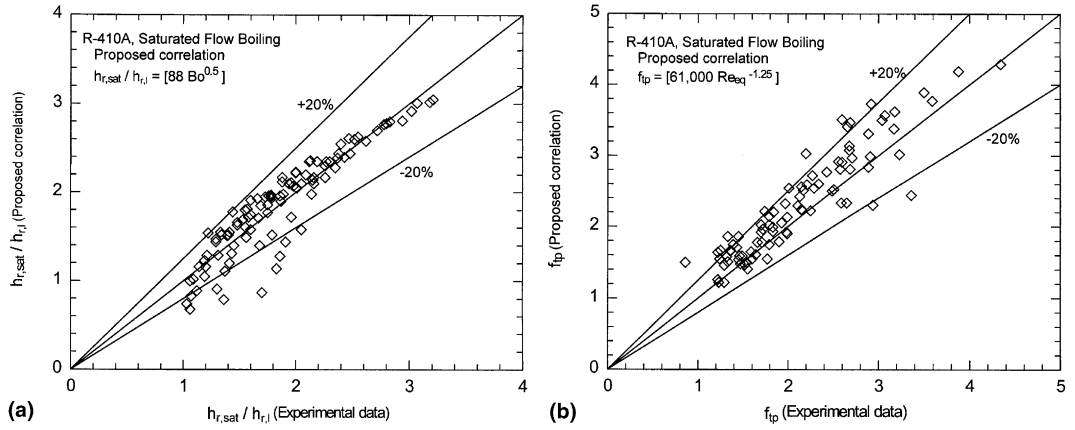

Fig. 9. Comparison of the proposed correlation with the present data for: (a) the heat transfer coefficient; (b) the friction factor.

$$h_{r,l} = 0.2092\left(\frac{k_l}{D_h}\right)Re^{0.78}Pr^{1/3}\left(\frac{\mu_m}{\mu_{wall}}\right)^{0.14} \tag{24}$$

and the boiling number is

$$Bo = \frac{q}{Gi_{fg}}. \tag{25}$$

Fig. 9(a) indicates that this correlation can satisfactorily correlate our data with an average deviation of 16.8%.

The measured frictional pressure drop is correlated in terms of the friction factor. According to our experimental data, the correlation for the friction factor f_{tp} is proposed as

$$f_{tp} = 61\,000Re_{eq}^{-1.25}, \tag{26}$$

where Re_{eq} is the equivalent Reynolds number and is defined as

$$Re_{eq} = \frac{G_{eq}D_h}{\mu_l} \tag{27}$$

in which

$$G_{eq} = G\left[(1 - X_m) + X_m\left(\frac{\rho_l}{\rho_g}\right)^{1/2}\right]. \tag{28}$$

Here G_{eq} is an equivalent mass flux which is a function of the R-410A mass flux, mean quality and density at the saturated condition. As seen in Fig. 9(b), 85% of the experimental data are correlated within 20%.

5. Concluding remarks

Experimental measurement has been carried out in the present study to investigate the saturated flow boiling heat transfer characteristics and pressure drop of R-410A in the vertical PHE. Results for the saturated flow boiling heat transfer coefficient and frictional pressure drop were examined in detail. In addition, correlation

equations were proposed to correlate the measured heat transfer and pressure data. The major results can be summarized in the following:

1. In the PHE, both the saturated flow boiling heat transfer coefficient and frictional pressure drop increase almost linearly with the imposed heat flux.
2. At a higher imposed heat flux, the effect of the refrigerant mass flux on the saturated flow boiling heat transfer coefficient is significant.
3. The system pressure shows relatively slight influence on the saturated flow boiling heat transfer coefficient. Nevertheless, a higher system pressure results in a lower frictional pressure drop.

Acknowledgements

The financial support of this study by the engineering division of National Science Council of Taiwan, ROC through the contract NSC 85-2221-E-009-06 is greatly appreciated.

References

[1] A.C. Talik, L.W. Swanson, L.S. Fletcher, N.K. Anand, Heat transfer and pressure drop characteristics of a plate heat exchanger, ASME/JSME Thermal Eng. Conf. 4 (1995) 321–329.
[2] A. Muley, R.M. Manglik, Experimental study of turbulent flow heat transfer and pressure drop in a plate heat exchanger with chevron plates, J. Heat Transfer 121 (1999) 110–117.
[3] B. Thonon, R. Vidil, C. Marvillet, Recent research and developments in plate heat exchangers, J. Enhanced Heat Transfer 2 (1995) 149–155.
[4] Y.Y. Yan, T.F. Lin, Evaporation heat transfer and pressure drop of refrigerant R-134a in a plate heat exchanger, J. Heat Transfer 121 (1999) 118–127.
[5] Y.Y. Yan, H.C. Lio, T.F. Lin, Condensation heat transfer and pressure drop of refrigerant R-134a in a plate heat exchanger, Int. J. Heat Mass Transfer 42 (1999) 993–1006.
[6] A. Cavallini, Review paper: working fluids for mechanical refrigerant invited paper presented at the 19th international congress of refrigerant, Int. J. Refrig. 19 (1996) 485–496.
[7] C.P. Yin, Y.Y. Yan, T.F. Lin, B.C. Yang, Subcooled flow boiling heat transfer of R-134a and bubble characteristics in a horizontal annular duct, Int. J. Heat Mass Transfer 43 (2000) 1885–1896.
[8] Y.Y. Yan, T.F. Lin, Evaporation heat transfer and pressure drop of refrigerant R-134a in a small pipe, Int. J. Heat Mass Transfer 41 (1998) 4183–4194.
[9] D. Graham, J.C. Chato, T.A. Newell, Heat transfer and pressure drop during condensation of refrigerant R-134a in an axially grooved tube, Int. J. Heat Mass Transfer 42 (1999) 1935–1944.
[10] H.J. Kang, C.X. Lin, M.A. Ebadian, Condensation of R134a flowing inside helicoidal pipe, Int. J. Heat Mass Transfer 43 (2000) 2553–2564.
[11] C.C. Wang, C.S. Chiang, Two-phase heat transfer characteristics for R-22/R-407C in a 6.5-mm smooth tube, Int. J. Heat Fluid Flow 18 (1997) 550–558.
[12] C.C. Wang, C.S. Chiang, D.C. Lu, Visual observation of two-phase flow pattern of R-22 R-134a and R-407C in a 6.5-mm smooth tube, Exp. Thermal Fluid Sci. 15 (1997) 395–405.
[13] C.Z. Wei, S.P. Lin, C.C. Wang, System performance of a split-type unit having R-22 and R-407C as working fluids, ASHRAE Trans. 120 (1997) 797–802.
[14] K. Cho, S.J. Tae, Evaporation heat transfer for R-22 and R-407C refrigerant–oil mixture in a microfin tube with a U-bend, Int. J. Refrig. 23 (2000) 219–231.
[15] T.Y. Choi, Y.J. Kim, M.S. Kim, S.T. Ro, Evaporation heat transfer of R-32, R-134a, R-32/134a and R-32/125/134a inside a horizontal smooth tube, Int. J. Heat Mass Transfer 43 (2000) 3651–3660.
[16] S.M. Sami, B. Poirier, Comparative study of heat transfer characteristics of new alternatives to R-22, ASHRAE Trans. 120 (1997) 824–829.
[17] S.M. Sami, B. Poirier, Two phase flow heat transfer of binary mixtures inside enhanced surface tubing, Int. Common. Heat Mass Transfer 25 (1998) 763–773.
[18] C.C. Wang, W.Y. Shieh, Y.J. Chang, Nucleate boiling performance of R-22, R-123, R-134a, R-410A and R407C on smooth enhanced tubes, ASHRAE Trans. 121 (1998) 1314–1321.
[19] T. Ebisu, K. Torikoshi, Heat transfer characteristics and correlations for R-410A flowing inside a horizontal smooth tube, ASHRAE Trans. 121 (1998) 556–561.
[20] H. Wijaya, M.W. Spatz, Two-phase flow heat transfer and pressure drop characteristics of R-22 and R-32/R125, ASHRAE Trans. 118 (1995) 1020–1027.
[21] J. Shen, K. Spindler, E. Hahne, Pool boiling heat transfer of refrigerant mixtures R-32/125, Int. Common. Heat Mass Transfer 26 (1999) 1091–1102.
[22] E.E. Wilson, A basic for traditional design of heat transfer apparatus, Trans. ASME 37 (1915) 47–70.
[23] S.J. Kline, F.A. McClintock, Describing uncertainties in single-sample experiments, Mech. Eng. 75 (1) (1953) 3–12.
[24] R.K. Shah, W.W. Focke, Plate heat exchangers and their design theory, in: R.K. Shah, E.C. Subbarao, R.A. Mashelkar (Eds.), Heat Transfer Equipment Design, Hemisphere, Washington, DC, 1988, pp. 227–254.
[25] J.G. Collier, Convective Boiling and Condensation, second ed., McGraw-Hill, New York, 1982.
[26] L.J. Chiang, Experimental study of saturated and subcooled flow boiling heat transfer of R-134a in plate heat exchanger, MS thesis, National Chaio Tung University, Hsinchu, Taiwan, ROC, 2000.